Saudi Journal of Biological Sciences 30 (2023) 103508

HOSTED BY

Contents lists available at ScienceDirect

Saudi Journal of Biological Sciences

journal homepage: www.sciencedirect.com

Original article

Alkaloid fraction of *Mirabilis jalapa Linn.* flowers has low cytotoxicity and increases iron absorption through Erythropoietin-Matriptase-2-Hepcidin pathway in iron deficiency Hepatocarcinoma cell model

Yuliana Heri Suselo [a,b,d], Dono Indarto [a,b,d,*], Brian Wasita [a,c], Hartono Hartono [a,b]

[a] Doctoral Program of Medical Sciences, Faculty of Medicine, Universitas Sebelas Maret, Surakarta, Indonesia
[b] Department of Physiology, Faculty of Medicine, Universitas Sebelas Maret, Surakarta, Indonesia
[c] Department of Anatomical Pathology, Faculty of Medicine, Universitas Sebelas Maret, Surakarta, Indonesia
[d] Biomedical Laboratory, Faculty of Medicine, Universitas Sebelas Maret, Surakarta, Indonesia

ARTICLE INFO

Article history:
Received 10 June 2022
Revised 25 October 2022
Accepted 11 November 2022
Available online 18 November 2022

Keywords:
M. jalapa flowers
Cytotoxicity
EPO
Hepcidin
Matriptase-2
Total iron

ABSTRACT

In this study, we investigated the effects of an alkaloid fraction of *Mirabilis jalapa* L. flowers in terms of cytotoxicity, Erythropoietin (EPO), hepcidin, and Matriptase-2 (MT-2) expression levels in iron deficiency Hepatocarcinoma (HepG2) cell model. The iron deficiency HepG2 cell model was generated by induction with Deferoxamine (DFO) and was then treated with standard therapy Ferric Ammonium Citrate (FAC) and different alkaloid fraction doses. Subsequently, the type II transmembrane serine proteases (TTSPs) activity and MT-2 expression were measured using a fluorometer and immunocytochemistry methods, while the EPO and hepcidin levels and total iron were examined using an ELISA kit and a colorimetric assay, respectively. The data were then analyzed using ANOVA with a significance level of 95 %. According to the UV–vis Spectrophotometry and HPLC results, the alkaloid fraction of *M. jalapa* flowers had 6.17- and 4-times higher Betaxanthin levels, respectively, compared to the ethanol extract of *M. jalapa* flower. Furthermore, LC-MS/MS analysis showed that the most dominant compound is Indicaxanthin. The ethanol extract and alkaloid fraction of *M. jalapa* flowers were not cytotoxic (IC_{50} > 30 ppm). Furthermore, the alkaloid fraction containing Indicaxanthin, Miraxanthin-V, and Boeravinone F is capable of increasing EPO levels, membrane and soluble TTSPs activity and MT-2 expression, decreasing hepcidin levels, and increasing intracellular iron levels in iron deficiency HepG2 cell model. In conclusion, the obtained alkaloid fraction of *M. jalapa* flowers has low cytotoxicity and the later increases iron absorption via EPO-MT2-hepcidin pathway in iron deficiency HepG2 cell model.
© 2022 The Author(s). Published by Elsevier B.V. on behalf of King Saud University. This is an open access article under the CC BY-NC-ND license (http://creativecommons.org/licenses/by-nc-nd/4.0/).

1. Introduction

Anemia remains a prominent nutritional challenge in both developed and developing countries (WHO, 2015). This hematological disorder is mainly caused by iron deficiency, and has a 25 % prevalence in the world's population. The highest number of cases has been reported in children (42.6 %), followed by pregnant women (38.2 %), and women of childbearing age (29 %) (Stevens et al., 2013). In Indonesia, the highest prevalence of anemia is in pregnant women (48.9 %), followed by children (38.5 %) (Agency of Health Research and Development, 2019).

The Indonesian government has implemented a 90-day iron supplementation program for pregnant women, which achieved a 95 % coverage rate in 2018. However, the prevalence of iron deficiency anemia (IDA) among pregnant women increased by 11.8 % in 2018, compared to 2013 (Agency of Health Research and Development, 2013, 2019). Several factors are responsible for the high prevalence of IDA, including non-adherence, negligence, or boredom in taking iron tablets, side effects, and unresponsiveness to iron tablets (Bregman et al., 2013; Suselo et al., 2017; Agency of Health Research and Development, 2019). In Indonesia, 61.8 % of

* Corresponding author at: Department of Physiology, Faculty of Medicine, Universitas Sebelas Maret, Surakarta, Indonesia.
E-mail addresses: yulianaheri@staff.uns.ac.id (Y.H. Suselo), dono@staff.uns.ac.id (D. Indarto), brianwasita@staff.uns.ac.id (B. Wasita), hartono65@staff.uns.ac.id (H. Hartono).
Peer review under responsibility of King Saud University.

Production and hosting by Elsevier

https://doi.org/10.1016/j.sjbs.2022.103508
1319-562X/© 2022 The Author(s). Published by Elsevier B.V. on behalf of King Saud University.
This is an open access article under the CC BY-NC-ND license (http://creativecommons.org/licenses/by-nc-nd/4.0/).

adolescent girls in Boyolali regency, Central Java have been reported to be unresponsive to oral iron therapy. It was shown that this population had higher hepcidin and lower matriptase-2 (MT-2) levels (Suselo et al., 2017), resulting in reductions of iron absorption within the small intestine, iron release from macrophages, and iron storage in the liver, and erythropoiesis (Fleming, 2008).

Several studies have been conducted in order to develop IDA therapies; for example, through activation of EPO-EPOR-MT2 complexes and hepcidin inhibition (Fung & Nemeth, 2013). Hepcidin antagonists may act by activation of Erythropoietin (EPO)–EPO Receptor (EPOR) complexes, expression inhibition, neutralization and inhibition of hepcidin–ferroportin (FPN) binding complexes (Hawula et al., 2019; Katsarou & Pantopoulos, 2018). Erythropoietin Stimulating Agent (ESA), for instance, is an EPO–EPOR complex agonist, which is known to have certain side-effects, including cardiovascular disorders and receptor resistance (Garrido et al., 2015; Rainville et al., 2016). In contrast to their unwanted effects, EPO agonists also have the capacity to increase MT-2 expression (Frýdlová et al., 2016), leading to inhibit interaction between Bone Morphogenetic Protein (BMP)-6 and BMP Receptor-1 (BMPR1) (Nai et al., 2016). Therefore, it will inhibit hepcidin expression, resulting in improvement of iron absorption (Camaschella et al., 2020). In addition, MT-2 agonists have not yet been established or developed. The MT-2 is a member of subfamily Type II transmembrane serine proteases (TTSPs), which are localized onto the cellular membranes of human cells. The active serine protease domain in the TTSPs has a catalytic-site triad at His^{57}, Asp^{102}, and Ser^{195} residues (chymotrypsin-like proteases). The human TTSPs family contains 17 protease members with several common structural features, including small *N*-terminal cytoplasmic, transmembrane, and stem domains, but only the MT-2 is involved in iron metabolism.

In silico and *in vitro* studies are commonly carried out for drug development. According to the results of biocomputational studies, *Indicaxanthin* is a potential EPO agonist, having dual effects as both an EPO–EPOR complex agonist and a BMPR-1 antagonist. As for other phytochemicals, *Miraxanthin V* is able to neutralize hepcidin and *Boeravinone F* is a hepcidin–ferroportin binding inhibitor, which is expected to increase intracellular iron absorption (Adiparadana et al., 2015; Suselo et al., 2017; Yotriana et al., 2018; Suselo et al., 2020). Furthermore, *Indicaxanthin, Miraxanthin V,* and *Boeravinone F* are members of the *Betaxanthin* group (alkaloid compounds) (Sadowska-Bartosz & Bartosz, 2021), which are commonly found in four o'clock flower plants (*Mirabilis jalapa* L.).

Primary and secondary cell lines are required for *in vitro* studies, focused on drug development. To investigate the effect of *Betaxanthin* group members on iron metabolism, we must use a human cell line with iron deficiency. Several hypoxia-mimetic agents, such as *Cobalt Chloride* ($CoCl_2$), *Dimethyloxalylglycine* (DMOG), and *Deferoxamine* (DFO) have been developed, but the mechanisms of the former two compounds in iron metabolism have not yet been established (Bedessem, 2015). The DFO has been widely used as a hypoxia-mimetic agent as well and affecting many proteins in iron metabolism at the cellular and systemic levels, and resulting in iron deficiency. From previous studies, 100 μM DFO has been found as the optimal concentration to induce iron deficiency and to increase MT-2 levels in several human cells lines, such as Caco-2, HepG2, HeLa, and MCF-7 (Bajbouj et al., 2018; Gulec and Gulec, 2018). In comparison with another iron chelator (*salicylaldehyde isonicotinoyl hydrazone*), DFO does not penetrate cell membranes and stabilizes MT-2 expression (Zhao et al., 2015). However, administration of any natural product as EPO-MT2 agonists and hepcidin antagonist has not been studied in an iron deficiency cell model. Therefore, in this study, we aimed to investigate the effects of an alkaloid fraction of *M. jalapa* flowers on cytotoxicity, EPO levels, TTSPs activity, MT-2 expression, hepcidin and iron levels in the iron deficiency HepG2 cell model.

2. Materials and methods

All materials used in this study were purchased from Thermofisher/Gibco, U.S. and Merck, Germany, unless otherwise stated.

2.1. Sample Collection

M. jalapa flowers were collected from the medicinal plant nursery center "Merapi Farma" in Sleman, Yogyakarta Province, Indonesia. Fresh flowers with a combination of yellow and pink color were then washed, sun-dried for 3 weeks, and oven-dried at 60 °C for 24 hours (h). Subsequently, the dried flowers were ground and sieved to obtain the powder.

2.2. Extraction and fractionation of M. jalapa flower

Powder of *M. jalapa* flowers was extracted using the maceration method with n-hexane (Merck, Germany) (1:10 weight/volume ratio). The residue was filtered and soaked in 96 % ethanol at a 1:10 v/v ratio for 6 days. Furthermore, the collected filtrates were evaporated at 45 °C for 1 h in a vacuum evaporator (IKA, Germany) and dried in an oven for 24 h (Maulina et al., 2018; Ministry of Health, 2017). Fractionation of the ethanol extract of *M. jalapa* flowers was adopted from an existing method, based on an acid–base method (dos Santos et al., 2013). The ethanol extract of *M. jalapa* flowers was dissolved in ethyl acetate (1:10 w/v ratio) and adjusted with 2 M HCl to reach a pH of 3. Then, NH_4OH was added to the separated acid layer, to a pH of 9. Finally, the collected ethyl acetate layers were evaporated using the vacuum evaporator at 45 °C for 4 h, then put in an oven at 45 °C for 24 h.

2.3. Identification of phytochemicals in M. jalapa extract and fraction

Each sample of extract and fraction of *M. jalapa* flowers was dissolved in ethanol and ethyl acetate solvents respectively and put into a 4.5 cm cuvette. The dissolved samples were spectrophotometrically measured using a U-2900 Shimadzu® at 480 nm and 535 nm for *Betaxanthin* and *Betacyanin* compounds, respectively. *Betaxanthin* and *Betacyanin* levels were quantified using the following formula (Mocanu et al., 2020):

$$\frac{Abs \times DF \times MW \times 1000}{\epsilon \times l}$$

where Abs represents the absorbance, DF signifies the dilution factor, MW denotes the molecular weight, ϵ indicates the molar extinction coefficient, and l denotes the cuvette length.

We confirmed the *Betaxanthin* and *Betacyanin* levels in the *M. jalapa* extract and fraction using the HPLC technique (Shimadzu, Japan) with *Betanin* (Sigma Aldrich, Singapore) as a standard. To detect these phytochemicals, we used a UV detector at 480 nm and 540 nm, respectively (Fernández-López et al., 2012). Furthermore, we evaluated the phytochemical contents in the *M. jalapa* fraction using an LC-MS/MS method. The mobile phase consisted of 7:3 v/v acetonitrile distillation in water and 10 mmol ammonium acetate. A total of 10 μL of sample was injected into the column, and the flow rate was adjusted at 1 mL/min (Maulina et al., 2018). The chromatogram and LC-MS/MS spectra were interpreted using the National Institute for Standard and Technology (NIST) (chemdata.nist.gov) and RIKEN MSn spectral database for phytochemicals (ReSpect) (spectra.psc.riken.jp).

2.4. Cytotoxicity assay of the ethanol extract and alkaloid fraction of M. jalapa flowers

For this assay, a HepG2 cell line obtained from The European Collection of Cell Cultures (ECACC, UK, Cat#85011430) was seeded

into passage 5 and cultured in Dulbecco's Modified Eagle Medium (DMEM) medium plus 2 mM L-glutamine, 200 U/mL penicillin, 200 mg/mL streptomycin, 1 mM sodium pyruvate, and 10 % heat-inactivated fetal bovine serum (FBS). A total of 10^4 cells/well were cultured in a 96-well plate and incubated under 37 °C, 95 % humidity, and 5 % CO_2 for 24 h (Béliveau et al., 2019). Once the HepG2 cells had confluenced, a cytotoxicity assay was performed using 2,5-diphenyl-2H-tetrazolium bromide (MTT) (Sigma, US) for 24 h (Xu et al., 2010). The number of viable cells was measured using a spectrophotometer with OD_{595}, followed by a 50 % Inhibitory Concentration (IC_{50}) calculation. The results of all treatments on HepG2 cell proliferation are expressed as a percentage (%) of viable cells, using the equation:

$$\%viablecells = \frac{ODtreatedcell - ODmedium}{ODcontrolcell - ODmedium} \times 100\%$$

The IC_{50} was determined by plotting the percentage of viable cells against AFF concentrations (ppm) to obtain a regression linear equation (probit analysis).

2.5. Generating iron deficiency cell model

To generate the iron deficiency cell model, HepG2 cells were induced by 100 μM DFO (Sigma, US), based on a previous study using Caco-2 and HepG2 cells (Gulec & Gulec, 2018). Initially, HepG2 cells were maintained in DMEM with 10 % FBS, 1 % non-essential amino acids, 1 % sodium pyruvate, and 1 % penicillin and streptomycin in a 5 % CO_2 incubator at 37 °C. Passage numbers of the cells were kept between 6 and 10, and confluenced HepG2 cells were plated in 6 wells, containing 10^5 cells/well, and were grown for 5 days post-confluence. The following day, the HepG2 cells were treated with 100 μM DFO and maintained in DMEM with 10 % FBS only for 24 h.

2.6. Study design of iron deficiency HepG2 cell model treated with alkaloid fraction of M. jalapa flowers

Iron deficiency HepG2 cell model was used to evaluate the effects of the alkaloid fraction of *M. jalapa* flowers (AFF) on MT-2 activity, hepcidin, and iron levels. In brief, we divided the HepG2 cells into 6 different groups: normal cells, iron deficiency cell model, which was induced with DFO (negative control = DFO), and treatment groups, which were treated with 100 μM FAC (positive control = DFO + FAC) and alkaloid fraction of *M. jalapa* flowers (DFO + AFF) at 0.5, 1, or 2 IC_{50} doses for 24 h. All experiments were performed in triplicate. A total of 10^6 of harvested HepG2 cells were separated into supernatants and pellets by centrifugation at 11.000 rpm for 10 min. The supernatants of cell medium were collected as soluble proteins and then were kept at − 80 °C. Meanwhile, the cell pellets were dissolved in 1 mL lysis buffer (Thermofisher, US) and extracted using a sonicator (OMNI, US) for 3 min. After centrifugation, the cleared solution was collected as the cell lysates, which represented as cell membrane and cytosol proteins and were kept in a − 80 °C for further analysis.

2.7. Measurement of EPO levels in iron deficiency HepG2 cell model

EPO levels in the supernatants from the 2.6 method section were quantified using a human EPO ELISA kit (ELK, China, Cat#ELK1011), based on the manufacturer's instructions. In brief, 10 μL of supernatants was dissolved in the sample buffer with a 1:5 v/v ratio and incubated with primary and secondary antibodies for 80 and 60 min respectively. The absorbance values were read using a spectrophotometer at 450 nm wavelength. The EPO levels in the supernatants of iron deficiency HepG2 cell model are presented as pg/mL.

2.8. Measurement of TTSPs activity in iron deficiency HepG2 cell model

The TTSPs activity was determined using the synthetic fluorescence substrate Boc-Gln-Ala-Arg-AMC (Sigma Aldrich, US), according to the existing method (Mangold et al., 2018). The substrate was dissolved in assay buffer (150 mM NaCl and 50 mM Tris pH 8.0) to reach a final concentration of 40 μM. The supernatants and cell lysates of all control and treatment groups were added to the substrate and incubated at 37 °C. The absorbance values were measured using a fluorometer (Glomax-Promega, US) at 365 nm emission wavelength and 460 nm excitation wavelength (Mangold et al., 2018). Finally, the TTSPs activity was determined using the Beer–Lambert Formula (expressed as IU/min) (Bisswanger, 2014).

2.9. Determination of Matriptase-2 expression in iron deficiency HepG2 cell model

An immunocytochemistry method was used to confirm the TTSPs activity results obtained by the above-mentioned method. For the immunostaining, we used 10^5 normal and iron deficiency HepG2 cells model, similar to the MT-2 activity study design, which were seeded into a 24-well plate with coverslips for 24 h. The following day, all HepG2 cells were incubated with 1:200 diluted monoclonal antibody anti-human MT-2 (Santa Cruz Biotechnology, US) for overnight. To detect MT-2 expression in the HepG2 cells, a secondary antibody conjugated streptavidin–horseradish peroxidase (Biocare, US) was used to generate antigen–antibody complexes. 3,3′-Diaminobenzidine (DAB) (Biocare, US) and Hematoxylin-Eosin (Merck, US) staining were used to visualize the presence of MT-2 protein in the HepG2 cells under a light microscope. Manual calculation of MT-2 expression was conducted, in a minimum of five fields, by two independent pathologists using the Image Raster software (https://www.miconos.co.id/p/download.html). The MT-2 expression is presented as the percentage of immunopositive cells divided by all iron deficiency HepG2 cells.

2.10. Measurement of Hepcidin levels in iron deficiency HepG2 cell model

Hepcidin levels in the supernatants and cell lysates were quantified using a human hepcidin ELISA kit (MyBioSource, US, Cat#MBS771863), based on the manufacturer's instructions. In brief, 10 μL of each supernatant or cell lysate was diluted with a dilution sample buffer in a1:5 ratio and incubated with primary and secondary antibodies. The absorbance values were read using a spectrophotometer at 450 nm wavelength. The hepcidin levels in the supernatants and cell lysates of iron deficiency HepG2 cell model are presented as ng/mL.

2.11. Measurement of iron levels in iron deficiency HepG2 cell model

Iron levels of supernatants and cell lysates were quantified using an iron assay kit (Sigma Aldrich, US), based on the manufacturer's instructions. To measure the total iron levels, 10 μL of each sample was added with 40 μL of iron assay buffer. The mixed samples were incubated for 60 min at 25 °C, then measured using a spectrophotometer at 595 nm wavelength. The total iron levels in supernatants and cell lysates of iron deficiency HepG2 cell model are presented as ng/μL.

2.12. Data analysis

All data were analyzed using the one-way ANOVA test with a significance level of 95 %, except for MT-2 expression, which was analyzed using the Kruskal–Wallis test.

3. Results

3.1. Phytochemical composition of the ethanol extract and alkaloid fraction of M. jalapa flowers

In this study, we are able to produce higher yields of ethanol extract and alkaloid fraction of *M. jalapa* flowers (Suppl.1). We then analyzed the *Betaxanthin* and *Betacyanin* levels in both the ethanol extract and alkaloid fraction of *M. jalapa* flowers. Fig. 1 shows that the *Betacyanin* levels (1,707.04 ± 20.16 ppm) were higher than the *Betaxanthin* levels (1,395.29 ± 14.40 ppm) in the alkaloid fraction, while they were lower than *Betaxanthin* levels (205.74 ± 19.16 vs 232.43 ± 12.10 ppm) in the ethanol extract. In addition, the *Betaxanthin* levels in the alkaloid fraction were 6.17 times greater than those in the ethanol extract ($p < 0.001$).

The standard curve, with serial doses of 200, 400, 600, and 1.000 ppm of *Betanin*, was used to calculate the *Betalain* levels (*Betaxanthin* and *Betacyanin*) in the ethanol extract and alkaloid fraction. Before measurement of *Betaxanthin* and *Betacyanin* levels, we evaluated the peak and retention time (rt) of *Betaxanthin* and *Betacyanin* using the standard compound *Betanin* at the wavelengths of 480 and 540 nm, respectively (Fig. 2).

We used the HPLC method to confirm quantification results of *Betaxanthin* and *Betacyanin* levels in the ethanol extract and alkaloid fraction of *M. jalapa* flowers (Suppl.2). It can be seen that the *Betaxanthin* in the ethanol extract and alkaloid fraction had slightly shorter rts than the standard compound. Meanwhile, the rts of *Betacyanin* in the ethanol extract and alkaloid fraction were similar to that of the standard compound. The alkaloid fraction had higher *Betaxanthin* and *Betacyanin* levels than the ethanol extract. In addition, the alkaloid fraction had 4 times higher *Betaxanthin* level, compared to the *Betacyanin* counterpart; meanwhile, the *Betaxanthin* levels in the ethanol extract were slightly higher than the *Betacyanin* counterpart. However, the *Betaxanthin* and *Betacyanin* levels determined using HPLC were lower than those obtained by UV–vis spectrophotometry (Fig. 1).

Table 1 lists the active compounds detected in the alkaloid fraction of *M. jalapa* flowers. We identified 15 phytochemicals that are alkaloid compounds, with various rts. The phytochemicals in the *Betaxanthin* group included *Indicaxanthin, Portulaxanthin, Lampranthin, Isolampranthin, Tryptophan-betaxanthin, Miraxanthin, Boeravinone F,* and *Vulgaxanthin,* which were more numerous than those in the *Betacyanin* group (i.e., *Betanin, Isobetanin, Betanidin,* and *Gomphrenin*). Furthermore, the peaks and rts of phytochemicals in the alkaloid fraction of *M. jalapa* flowers are depicted in the LC-MS/MS chromatogram in Fig. 3. The highest peak was that of *Indicaxanthin*, followed by *Gomphrenin I* and *Boeravinone F.*

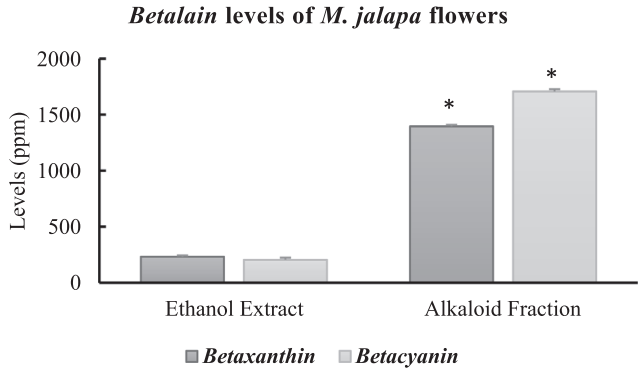

Fig. 1. *Betaxanthin* and *Betacyanin* levels found in the ethanol extract and alkaloid fraction of *M. jalapa* flowers. This measurement was determined using a UV–vis Spectrophotometer. All experiments were performed in duplicate, and * designates comparisons between *Betaxanthin/Betacyanin* levels in ethanol extract and alkaloid fraction with $p < 0.001$.

3.2. Cytotoxicity effects of the ethanol extract and alkaloid fraction of M. jalapa flowers in HepG2 cells

The MTT assay was used to analyze the cytotoxicity of the alkaloid fraction of *M. jalapa* flowers. Table 2 indicates that the alkaloid fraction had a lower IC_{50} value than the ethanol extract (100.21 ± 5. 67 vs 187.79 ± 4.13 ppm, respectively). The graph of MTT assay was indicated in Fig. 4.

3.3. EPO levels in iron deficiency HepG2 cell model

To evaluate the role of EPO protein in the iron regulation through the EPO-MT-2-hepcidin complexes pathway, we measured the EPO levels in DFO, DFO + FAC and DFO + AFF groups. Fig. 5 shows that the EPO levels increased in the supernatants of DFO + FAC and DFO + AFF, higher than that of DFO group. The average of EPO levels in DFO + FAC (1,471.63 ± 75.82 pg/mL), DFO + 1IC_{50} and DFO + 2 IC_{50} (1,368.75 ± 14.70 and 1,562.70 ± 59.12 pg/mL, respectively) groups were significant higher than the average of EPO levels in the DFO group (1,235.27 ± 49.50 pg/mL; $p < 0.05$). The higher increased EPO levels associated with the higher AFF doses.

3.4. TTSPs activity in iron deficiency HepG2 cell model

To confirm interaction between EPO and EPOR, we measured TTSPs activity and MT-2 expression. In Fig. 6, we evaluated the activity of TTSPs protein in the supernatants and cell lysates of iron deficiency HepG2 cell model. In the HepG2 normal cells, TTSPs activity was only observed in the supernatants (3.44 ± 0.45 IU/mi n). The TTSPs activity in the cell lysates (2.64 ± 0.22 IU/min) and supernatants (4.62 ± 0.10 IU/min) of DFO group were significantly higher than in the cell lysates and supernatant of HepG2 normal cells ($p < 0.001$). After treatment with 100 and 150 μM FAC, the TTSPs activity significantly decreased in the cell lysates (0.63 ± 0.01 and 0.13 ± 0.02 IU/min, respectively) and supernatants (0.16 ± 0.03 and 0.08 ± 0.00 IU/min, respectively) of DFO group ($p < 0.001$). Interestingly, administration of 0.5, 1, and 2 IC_{50} doses of AFF to DFO group increased TTSPs activity in a dose-dependent manner, with significant differences compared to the TTSPs activity in DFO group. Furthermore, significantly higher TTSPs activity in the cell lysates were observed in DFO + 0.5, 1, and 2 IC_{50} doses of AFF, compared to that in DFO group. DFO + 2 IC_{50} AFF dose had similar supernatants TTSPs activity as DFO group, while DFO + 0.5 IC_{50} AFF and DFO + 1 IC_{50} AFF had lower supernatants TTSPs activity than DFO group.

3.5. Matriptase-2 expression in iron deficiency HepG2 cell model

We verified the TTSPs activity results in the cell lysates and supernatants of iron deficiency HepG2 cell model by performing immunocytochemistry with the antibody anti-MT-2 protein (Fig. 7). HepG2 normal cells did not express MT-2 protein, while the DFO group expressed 5.5 % MT-2 proteins (Table 3). With a similar pattern as TTSPs activity, administration of 100 μM FAC also reduced the MT-2 expression in DFO+FAC group. Administration of 0.5, 1, or 2 doses of AFF significantly increased MT-2 expres-

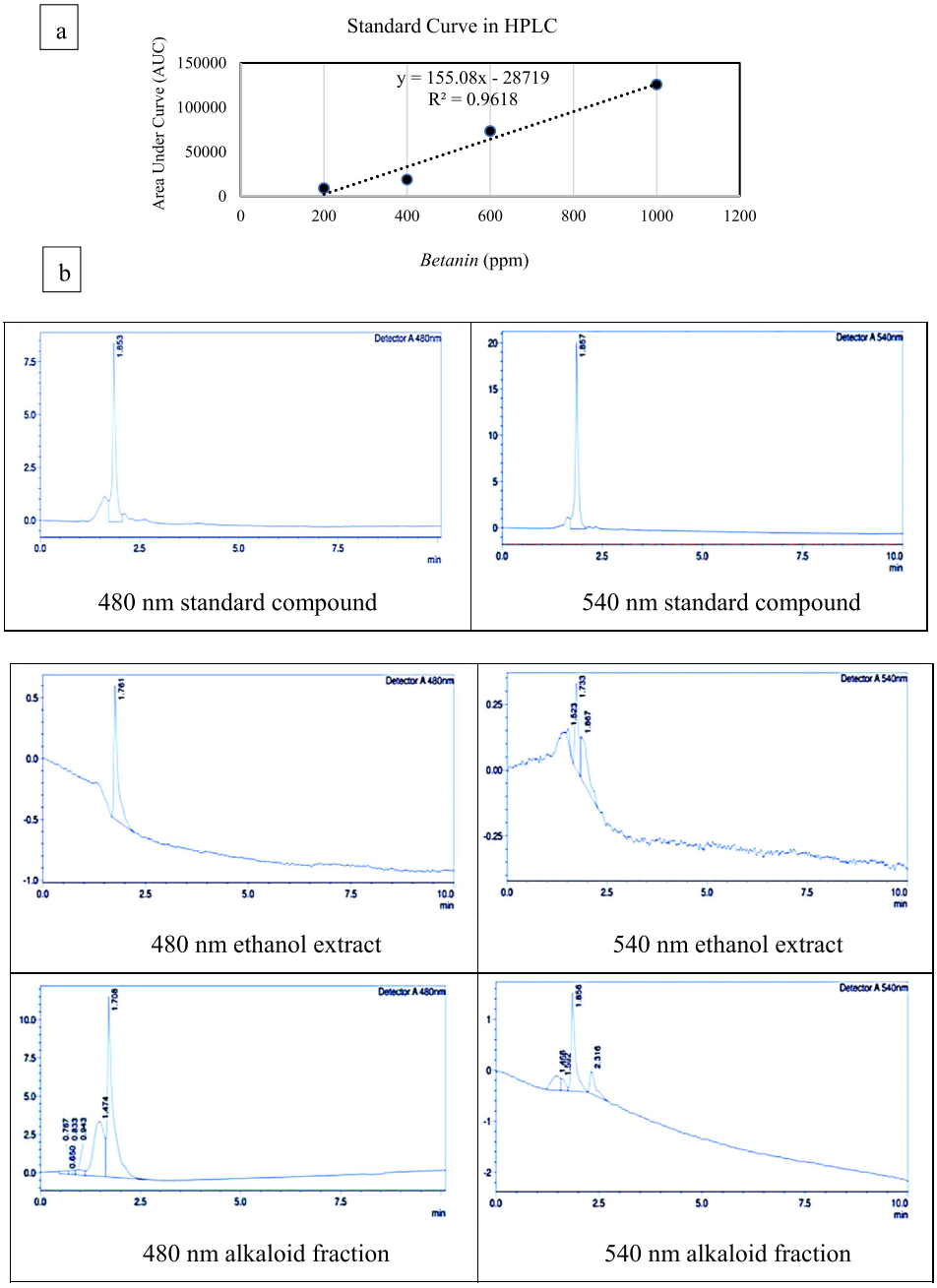

Fig. 2. (a) The standard curve of *Betanin* using HPLC. *Betanin* is the precursor of the phytochemical compounds *Betaxanthin* and *Betacyanin*; (b) Chromatographs of the standard compound, as well as the ethanol extract and alkaloid fraction of *M. jalapa* flowers, using HPLC analysis the wavelengths 480 and 540 nm.

sion in DFO+AFF groups, when compared to that in DFO group. Furthermore, significant differences in MT-2 expression were found between 1 and 2 IC_{50} doses of DFO + AFF groups ($p < 0.001$).

3.6. Hepcidin levels in iron deficiency HepG2 cell model

To examine changes in EPO levels, TTSPs activity, and MT-2 expression in iron deficiency HepG2 cell model, we also measured the level of hepcidin, which is a downstream protein in the EPO-MT-2-hepcidin pathway. Fig. 8 shows the hepcidin levels in the cell lysates and supernatants of iron deficiency HepG2 cell model treated with FAC and AFF. The highest hepcidin levels were detected in the cell lysate (57.67 ± 0.83 ng/mL) and supernatant (57.25 ± 1.78 ng/mL) of HepG2 normal cells. DFO group had significantly lower hepcidin levels, either in cell lysate or supernatant, than their counterpart in HepG2 normal cells ($p = 0.001$). Administration of 100 μM FAC and 0.5, 1, or 2 IC_{50} AFF significantly reduced hepcidin levels in cell lysates and supernatants of iron deficiency HepG2 cell model ($p < 0.001$). The lowest levels of hepcidin were detected in DFO + 2 IC_{50} AFF group. In addition, the hepcidin levels in the supernatant of DFO group were significantly higher than those observed in DFO + FAC, DFO + 1 IC_{50} AFF, and DFO + 2 IC_{50} AFF groups.

3.7. Total iron levels in iron deficiency HepG2 cell model

Measurement of total iron levels was carried out to further analyze changes in EPO-MT-2 and hepcidin expression with respect to

Table 1
Phytochemicals identified in alkaloid fraction of *M. jalapa* flowers using LC-MS/MS analysis.

No	Phytochemicals	retention time (rt) (min)	MS (M^+H^+) (*m/z*)	Molecular Weight	Molecular Formula
1.	*Indicaxanthin*	0.317	316.40	308	$C_{14}H_{16}N_2O_6$
2.	*Portulaxanthin III*	1.036	256.43	269	$C_{11}H1_2N_2O_6$
3.	*Lampranthin II*	3.889	701.70	726	$C_{34}H_{34}N_2O_{16}$
4.	*Isolampranthin II*	4.326	702.80	726	$C_{34}H_{34}N_2O_{16}$
5.	*Tryptophan-betaxanthin*	4.660	397.11	398	$C_{20}H_{19}N_3O_6$
6.	*Boeravinone F*	6.768	318.61	326	$C_{17}H_{10}O_7$
7.	*Miraxanthin V*	8.952	343.56	346	$C_{17}H_{18}N_2O_6$
8.	*Betanin*	10.957	550.59	550	$C_{24}H_{26}N_2O_{13}$
9.	*Isobetanin*	11.959	537.66	550	$C_{24}H_{26}N_2O_{13}$
10.	*Vulgaxanthin I*	15.326	279.56	339	$C_{14}H_{17}N_3O_{17}$
11.	*Miraxanthin I*	16.302	353.44	358	$C_{14}H_{18}N_2O_7S$
12.	*Miraxanthin II*	17.760	239.47	326	$C_{13}H_{14}N_2O_8$
13.	*Betanidin*	18.307	381.58	388	$C_{18}H_{16}N_2O_8$
14.	*Gomphrenin II*	19.361	621.63	696	$C_{33}H_{32}N_2O_{15}$
15.	*Gomphrenin I*	21.237	576.20	550	$C_{24}H_{26}N_2O_{13}$

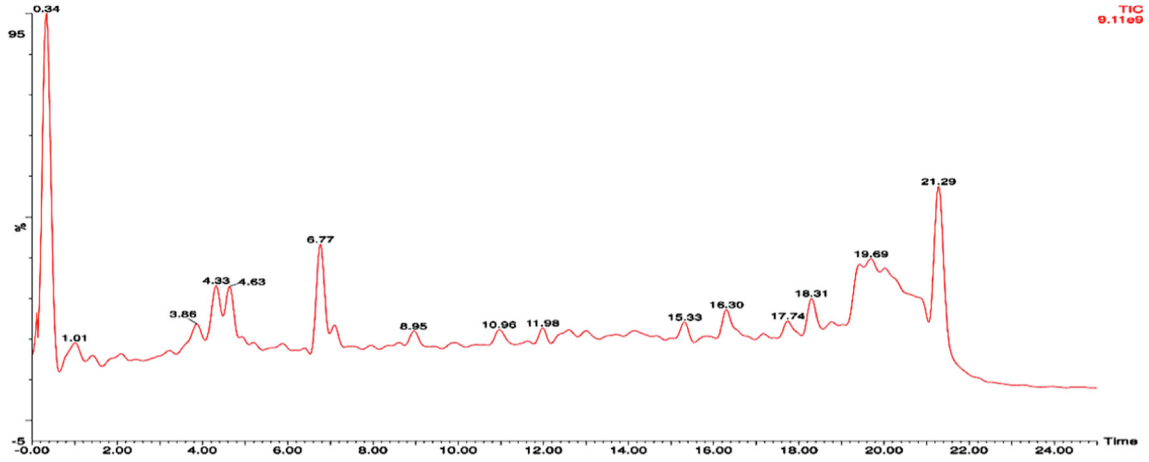

Fig. 3. Chromatogram of the alkaloid fraction of *M. jalapa* flowers using LC-MS/MS analysis. A 10 µL alkaloid fraction was injected into the column using 7:3 acetonitrile distillation in water and 10 mmol ammonium acetate. Fractionated samples were collected into 3 mL tubes with flow rate at 1 mL/min. The phytochemical analysis was performed in triplicate and the above chromatogram represents three independent experiments.

Table 2
IC_{50} doses for ethanol extract and alkaloid fraction of *M. jalapa* flowers.

MTT assay	Ethanol extract (ppm)	Alkaloid fraction (ppm)	p-value
Mean ± SD	187.79 ± 4.13	100.21 ± 5.67	<0.001

Note: All experiments were performed in triplicate.

iron uptake in iron deficiency HepG2 cell model (Fig. 9). In the HepG2 normal cells, an iron level of 1.97 ± 0.23 ng/µL was found in the cell lysate, much higher than the supernatant. Administration of 100 µM DFO in HepG2 cells (DFO group) reduced the iron level by half in the cell lysate, but almost did not affect that in the supernatant. Treatment with 100 µM FAC in DFO+FAC group significantly increased iron levels (1.42 ± 0.35 ng/µL), 1.5 times higher than that in the cell lysate of DFO group (0.93 ± 0.34 ng/µL); meanwhile, the iron level in the supernatant was around 7 times higher, compared to the supernatant in DFO group. In contrast to these results, the iron levels in the cell lysate of DFO group treated with 0.5, 1, and 2 IC_{50} AFF was significantly increased in a

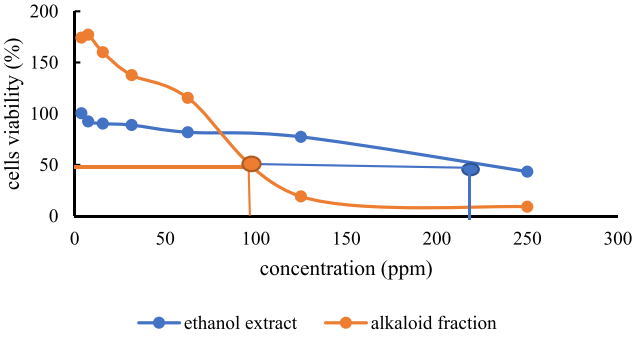

Fig. 4. The cytotoxic effect of ethanolic extract and alkaloid fraction of *M. jalapa* flowers. A total of 10^5 HepG2 cells were seeded in a 96-well microplate for 24 h and then incubated with 7 serial dilutions of the alkaloid fraction with MTT reagent from 3.9 to 250 ppm for 24 h. The following day, the 10 % SDS in 0.1 N HCl stop solution was added into each well of iron deficiency HepG2 cell model for overnight and the formazan formation in HepG2 cells was spectrophotometrically measured at 595 nm wavelength. The IC_{50} was determined by plotting the percentage of viable cells against AFF concentrations (ppm) using probit analysis. All experiments were performed in triplicate.

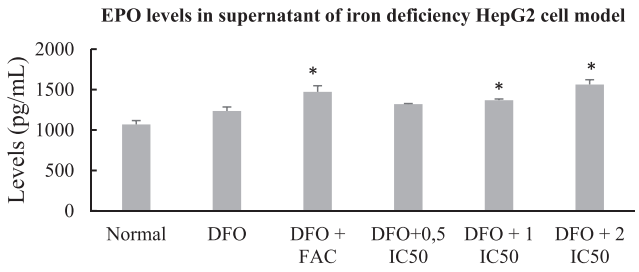

Fig. 5. EPO levels in supernatants of iron deficiency HepG2 cell model treated with FAC and AFF. A total of 10^5 HepG2 cells were seeded in a six-well microplate for 24 h and were then induced with 100 μM DFO for 24 h (DFO group). The following day, the DFO group was treated with 100 μM FAC and 0.5, 1, or 2 IC_{50} AFF. All experiments were performed in triplicate. *denotes comparison between the DFO group and FAC/AFF treated DFO groups with $p < 0.05$. The HepG2 normal cells provided the baseline data and were compared to the DFO group.

dose-dependent manner, when compared to the DFO group. The highest cell lysate iron level (6.70 ± 0.03 ng/μL) was observed in the DFO + 2 IC_{50} AFF group. The iron levels in the supernatants of those cells remained stable, compared to those in the DFO group.

4. Discussion

4.1. Alkaloid fraction of M. jalapa flowers has higher Betacyanin and Betaxanthin levels than ethanol extract of M. jalapa flowers

We used a maceration technique for extraction of *M. jalapa* flowers because all members of the *Betalain* family (including *Betaxanthin* and *Betacyanin*) are thermolabile compounds but we needed longer times to generate the 17.50 % extract of *M. jalapa* flowers. Only one study stated that fresh flowers of *M. jalapa* contain more phytochemicals, compared to other parts of the same plant (Piattelli et al., 1965). In comparison with leaves and roots extraction, we are unable to compare to the yields of our study since the existing studies used the *M. jalapa* plants from different environmental growth area, isolation methods, harvest time, and chemicals solvent for extraction (Gogoi et al., 2016; Maulina et al., 2018). We further fractionated the ethanol extract of *M. jalapa* flowers and obtained the 20.89 % alkaloid fraction. *Betaxanthin* and *Betacyanin* levels increased by 6.17 and 8.33 times respectively in the alkaloid fraction, compared with the ethanol extract.

Generally, *Betalains* are found in pigmented plants, such as *Bougainvillea*, *Caryophyllales*, *Amaranthin*, and Beets; however, the *Betaxanthin* and *Betacyanin* levels vary among these plants (Fernández-López et al., 2012; Khan & Giridhar, 2015; Lavanya et al., 2019; Naqvi and Husnain, 2020). *Betacyanin* levels are commonly higher than *Betaxanthin* levels in *Pear cactus* and *Bougainvillea* (Coy-Barrera, 2020). Conversely, the *Betaxanthin* levels in our study were 4 times higher than *Betacyanin* levels in the obtained alkaloid fraction (with 1.76 and 1.71 min rt at 480 nm, respectively). This result indicates that the alkaloid fraction of *M. jalapa* flowers is a better source of *Betaxanthin*.

The phytochemicals which belong to the *Betaxanthin* group in our results differed from those reported in a previous study using fresh *M. jalapa* flowers. They reported that *Indicaxanthin, Vulgaxanthin-I,* and *Miraxanthin-I, -II, -III, -IV, -V* and *-VI* were identified in fresh *M. jalapa* flowers (Ali Esmail Al-Snafi et al., 2021), while we only found *Indicaxanthin, Vulgaxanthin-I,* and *Miraxanthin I, II,* and *V* in our alkaloid fraction. Interestingly, we detected more other phytochemicals than previous studies (Table 1). Based on the color of the flower, red petals of *M. jalapa* flowers have been shown to contain *Betanin, Isobetanin, Neobetanin, Betanidin, Lampranthin II, Miraxanthin-V, Miraxanthin-III,* and *3-methoxytyramine-betaxanthin,* while yellow petals contain *Indicaxanthin, Miraxanthin-III,* and *3-methoxytyramine-betaxanthin* (Polturak et al., 2018). As we used a combination of yellow and pink *M. jalapa* flowers in our study (Suppl.3), almost all phytochemicals mentioned above were identified. In contrast to our study, a previous study using an extract from leaves of Indonesian *M. jalapa* has identified 30 phytochemicals, including *Indicaxanthin, Miraxanthin, Boeravinone*, and some non-*Betaxanthin* phytochemicals (Maulina et al., 2018).

4.2. Ethanol extract and alkaloid fraction of M. jalapa flowers have low cytotoxicity in iron deficiency HepG2 cell model.

According to the National Cancer Institute, crude extracts have high toxicity to human cell lines if the IC_{50} is<30 ppm (Livingstone, 2001). Our findings showed that ethanol extract and alkaloid fraction of *M. jalapa* flowers have 187.79 and 100.21 ppm respectively, which exhibit low toxicity to HepG2 cells. In contrast, another study reported that Ribosome-Inactivating Protein (RIP) isolated from *M. jalapa* leaves are toxic to T47D, SiHa, and mononuclear cells, with IC_{50} values of 0.36, 5.6, and 21.04 ppm, respectively (Ikawati et al., 2006). Meanwhile, another pure compound *Mirabijalone* derivative from *M. jalapa* roots, had various IC_{50} values ranging from < 5 to > 100 ppm in SKBR-3, HeLa, and WI-38 cell lines (Sharathna et al., 2021). In addition to the cytotoxicity of phyto-

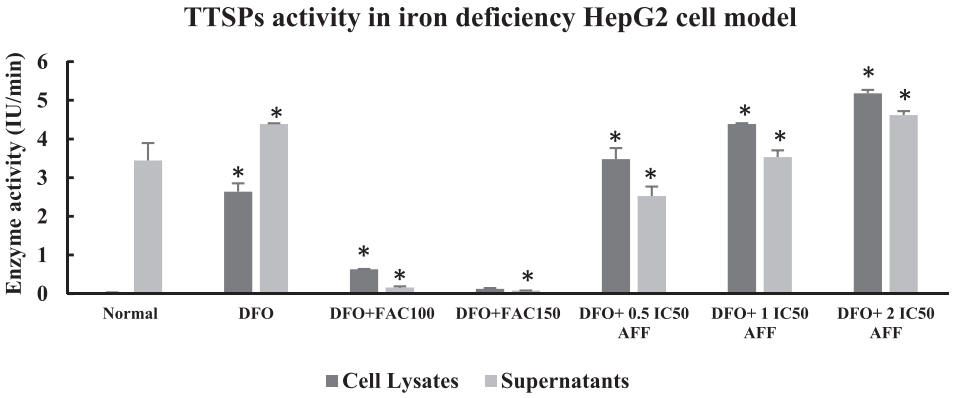

Fig. 6. TTSPs activity in lysates and supernatants of iron deficiency HepG2 cell model treated with FAC or AFF. A total of 10^5 HepG2 cells were seeded in a six-well microplate for 24 h, then induced with 100 μM DFO for 24 h (DFO group). The following day, the DFO group was treated with 100 μM FAC and 0.5, 1, or 2 IC_{50} AFF. Cell lysates and supernatants of HepG2 normal cells, DFO group, and FAC/AFF treated-DFO groups were added to 40 μM of Boc-Gln-Ala-Arg-AMC substrate. All experiments were performed in triplicate. *denotes comparison between the DFO group and treated DFO groups with $p < 0.001$. The HepG2 normal cells provided the baseline data and were compared to the DFO group.

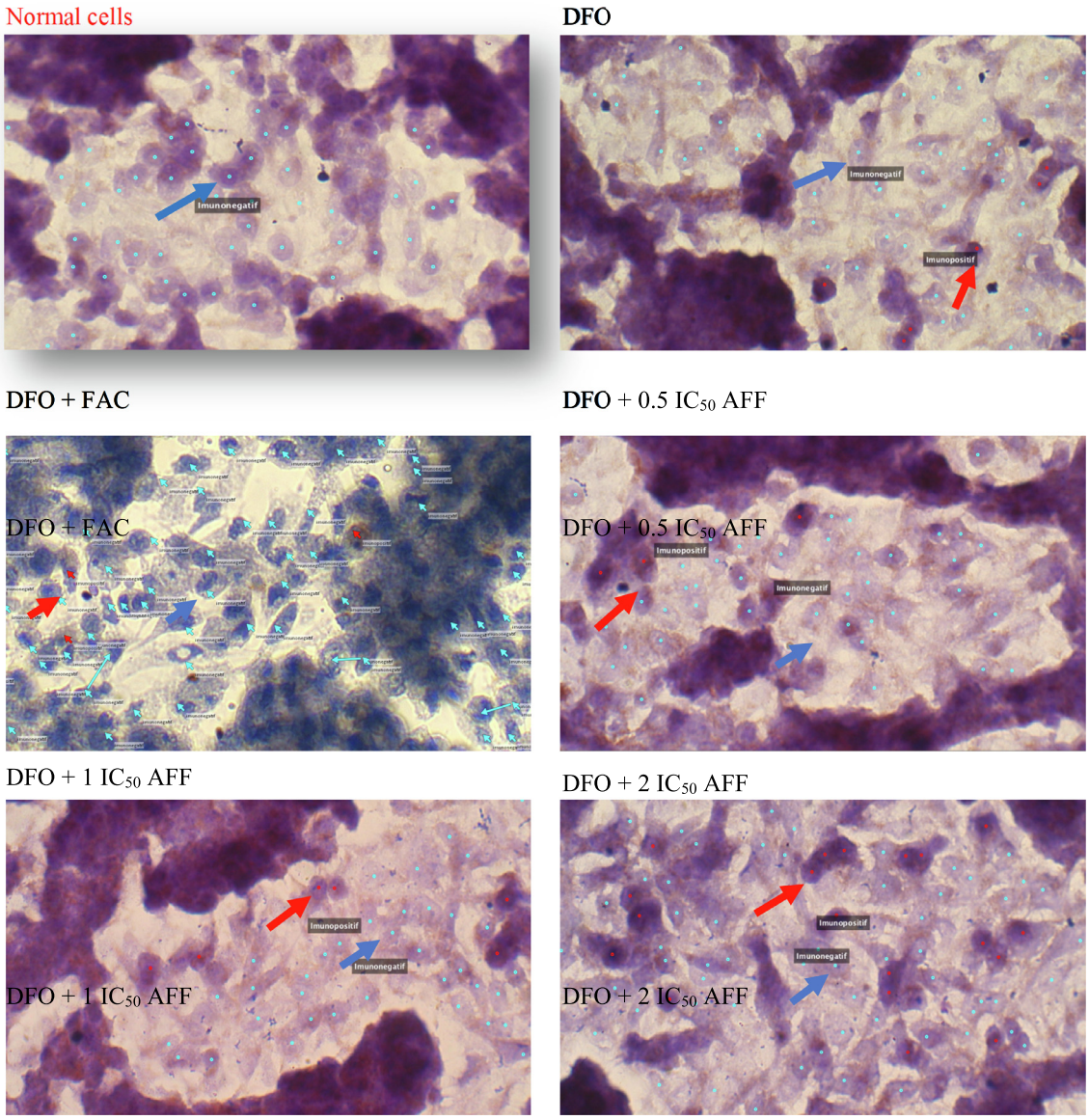

Fig. 7. Results of MT-2 expression in DFO group and DFO treated with 100 μM FAC and 0.5, 1, or 2 IC_{50} AFF groups. A total of 10^5 HepG2 cells were grown in the coverslip of a 24-well microplate for 24 h, then induced with 100 μM DFO for 24 h (DFO group). The following day, the DFO group was treated with 100 μM FAC and 0.5, 1, or 2 IC_{50} AFF. HepG2 normal cells, DFO group, and FAC/AFF treated-DFO groups were stained with monoclonal antibody anti-human MT-2 and secondary antibody conjugated streptavidin–horseradish peroxidase. All experiments were performed in duplicate. Red arrow: immunopositive; Blue arrow: immunonegative. The HepG2 normal cells provided the baseline data and were compared to the DFO group.

Table 3
Percentage of iron deficiency HepG2 cell model positively expressing MT-2 proteins.

MT-2 Expression (%)	Normal	DFO	DFO+ FAC	DFO+ 0.5 IC_{50}	DFO + 1 IC_{50}	DFO+ 2 IC_{50}	p-value
Mean	0	5.52	2.91	3.13	9.16	13.47	<0.001
SD	0	2.12	1.74	0.43	0.12	0.90	

chemicals from *M. jalapa* roots, several studies using *Boeravinone* isolated from *M. jalapa* roots have reported IC_{50} values of 0.92 in K562 cells, >100 in HL-60 cells, 9.62 in A549 cells, and 2.16 in BEL-7402 cells (Xu et al., 2010). Therefore, the low cytotoxicity of the ethanol extract and alkaloid fraction of *M. jalapa* flowers in this paper may be due to the combination of many phytochemicals, human cell line preference and different parts of *M. jalapa* plant, leading to antagonistic effects.

4.3. Alkaloid fraction of M. jalapa flowers increases EPO levels in supernatants of the iron deficiency HepG2 cell model

A previous *in silico* study has identified that *Indicaxanthin, Miraxanthin V,* and *Vulgaxanthin I* are able to interact with EPOR with lower binding affinity than EPO–EPOR complexes and having molecular structures similar to the truncated EPO ptoteins (Suselo et al., 2017). From our *in vitro* results, the EPO levels in cell lysates

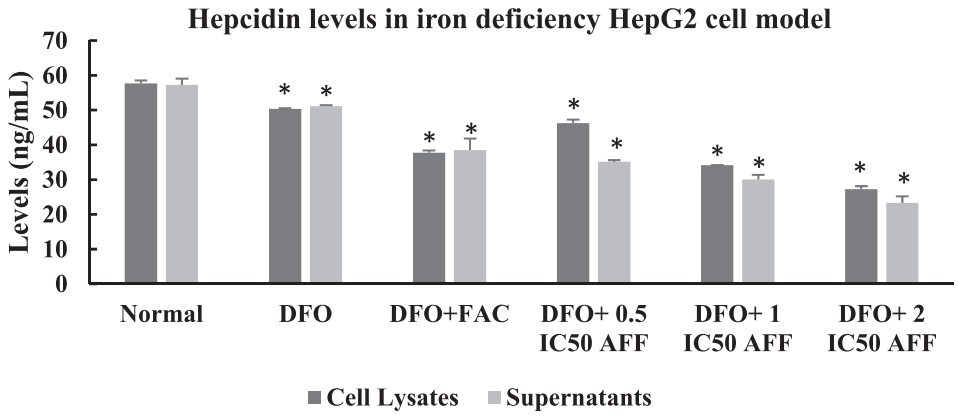

Fig. 8. Hepcidin levels in cell lysates and supernatants of iron deficiency HepG2 cell model treated with FAC and AFF. A total of 10^5 HepG2 cells were seeded in a six-well microplate for 24 h, then induced with 100 μM DFO for 24 h (DFO group). The following day, the DFO group was were treated with 100 μM FAC and 0.5, 1, or 2 IC_{50} AFF. All experiments were performed in triplicate. *denotes comparison between the DFO group and FAC/AFF treated DFO groups with $p < 0.001$. The HepG2 normal cells provided the baseline data and were compared to the DFO group.

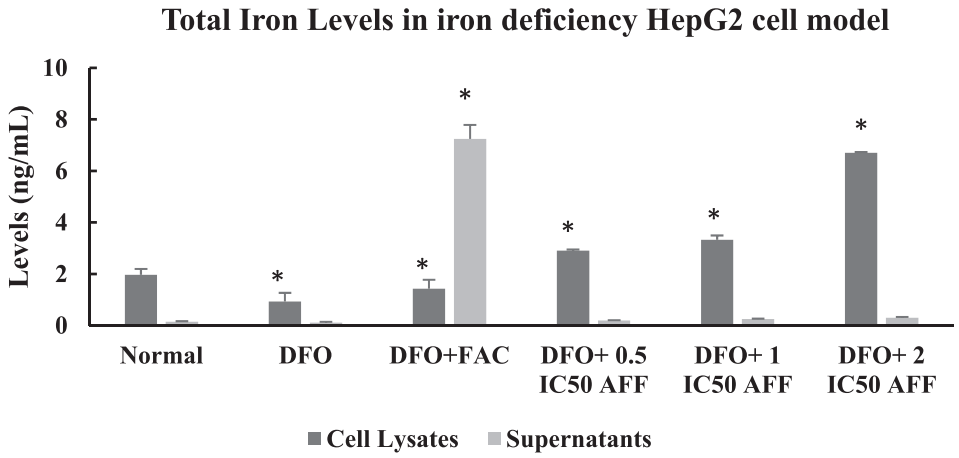

Fig. 9. Total iron levels in cell lysates and supernatants of iron deficiency HepG2 cell model treated with FAC and AFF. A total of 10^5 HepG2 cells were seeded in a six-well microplate for 24 h, then induced with 100 μM DFO for 24 h (DFO group). The following day, the DFOgroup was treated with 100 μM FAC and 0.5, 1, or 2 IC_{50} AFF. All experiments were performed in triplicate. *denotes comparison between the DFO group and FAC/AFF treated DFO groups with $p < 0.001$. The HepG2 normal cells provided the baseline data and were compared to the DFO group.

and supernatants of the iron deficiency HepG2 cell model increased in a dose-dependent manner after administration of the alkaloid fraction of *M. jalapa* flowers (Fig. 5). In addition to this *in vitro* study, administration of EPO in mice and rats with iron deficiency increases MT-2 gene expression (Frýdlová et al., 2016). Altogether, it suggests that administration of the alkaloid fraction of *M. jalapa* flowers probably increases the TTSPs activity and MT-2 expression through interaction with EPOR as well. However, further studies are required to determine the expression changes of EPOR in the iron deficiency HepG2 cell model.

4.4. Alkaloid fraction of M. jalapa flowers increases TTSPs activity in cell lysates and supernatants of the iron deficiency HepG2 cell model

There are two types of TTSPs (i.e., membrane and soluble enzymes), which possess single pass transmembrane, short intracellular and extracellular domains. The TTSPs catalytic site activates or degrades protease-activated receptors, cytokines, growth factors and extracellular matrix components (Webb et al., 2011). The MT-2 protein is a family member of TTSPs also has membrane and soluble enzymes which have a specific catalytic site at His^{57}, Asp^{102}, and Ser^{195} residues, and shares 45 % sequence homology to other members of TTSP family. Meanwhile, the Arg-Ile-Val-Gln-Gly sequence of MT-2 protein has an important role for zymogen activation (Mangold et al., 2018). Basically, 2 types of the MT-2 protein have similar TTSPs activity but the soluble form lacks of the extracellular domain (Stirnberg et al., 2010). We used the Boc-Gln-Ala-Arg-AMC substrate, which is only the fluorogenic tripeptide available in the market, for which the MT-2 protein is able to cleave Arg at *P*1, *P*2 or *P*3, and *P*4 positions. The cleavage of the substrate (AMC) results in fluorescence (Mangold et al., 2018). These findings emphasize that the Boc-Gln-Ala-Arg-AMC substrate can be cleaved by other members of TTSP family which have the same catalytic triad (His_{57}, Asp_{102}, and Ser_{195}) (Damalanka & Janetka, 2019; Rawlings, 2020); however, MT-2 protein shows the highest expression of the TTSPs family in the cell membrane of HepG2 (https://www.proteinatlas.org/search/type+2+transmembrane+protease+serine), such that the TTSPs activity may derive from the presence of MT-2 protein.

4.5. Alkaloid fraction of M. jalapa flowers increases matriptase-2 expression in cell lysates and supernatants of the iron deficiency HepG2 cell

To verify the TTSPs activity in iron deficiency HepG2 cell model treated with the alkaloid fraction of *M. jalapa* flowers, we evaluated

MT-2 protein expression. Increased expression of MT-2 was found to be parallel with increased TTSPs activity in iron deficiency HepG2 cell model treated with the alkaloid fraction of *M. jalapa* flowers in a dose-dependent manner. These findings clearly indicate that the alkaloid fraction of *M. jalapa* flowers was able to induce MT-2 protein expression and increase TTSPs activity. The results of this *in vitro* study confirm that *Indicaxanthin* and *Miraxanthin-V* from *in silico* study have lower binding affinity (-4.50 and −5.03 kcal/mol resppectively) than the standard EPO (-3.80 kcal/mol). In addition, both phytochemicals similarly interact with EPOR at Leu^{33}, Glu^{34}, Glu^{60}, Asp^{61}, Thr^{87}, Ala^{88}, Thr^{90}, and Ser^{92} residues but both phytochemicals have additional interaction at Phe^{93}, His^{114}, Glu^{117}, and Phe^{205} residues. Interaction with Met^{150} and Phe^{205} residues are necessary for EPOR binding like Epo-mimetic peptide (EMP1) (Middleton et al., 1999). Furthermore, interaction with Phe^{93} residue plays an important role in nonpolar interactions with EPOR (Singh et al., 2013). The other 10 residues are required for bond stability of phytochemicals to EPOR (Suselo et al., 2017). In previous study, EPO administration in rats increases splenic erythroferrone (ERFE) protein and liver TMPRSS6 protein expression. Furthermore, HAMP expression in animals treated with the combination of iron plus EPO is significantly lower than HAMP expression in animals treated with iron alone (Gurieva et al., 2017). Therefore, administration of alkaloid fraction of *M. jalapa* flowers may increase TTSPs activity and MT-2 expression but further studies are required to understand the association and dissociation affinities between phytochemicals in the alkaloid fraction with EPOR.

4.6. Alkaloid fraction of M. jalapa flowers inhibits hepcidin levels in cell lysate and supernatant of the iron deficiency HepG2 cell model

Iron deficiency in HepG2 cells induces MT-2 expression, which stabilizes at the cytoplasmic domain to cleave hemojuvelin protein and inhibit BMP 2 and BMP6 protein complexes from interacting with BMPR (Zhao et al., 2015). Inhibition of BMP–BMPR complexes result in the inhibition of HAMP (hepcidin) gene expression (Camaschella et al., 2020). The results of our study showed that hepcidin levels in the cell lysate and supernatant of HepG2 cells were reduced significantly after administration of the alkaloid fraction of *M. jalapa* flowers in a dose-dependent manner. From an existing *in vitro* study, some synthetic compounds have been shown to inhibit MT-2 and HJV gene and protein expression, as well as activating HAMP gene and hepcidin levels (Béliveau et al., 2019). Therefore, it suggests that hepcidin expression is, at least partly, regulated by the MT2–BMP pathway.

4.7. Alkaloid fraction of M. jalapa flowers increases iron levels in cell lysate of the iron deficiency HepG2 cell model

Iron is a vital trace mineral that plays important roles in enzymatic reactions, especially in mitochondrial human cells, such as hepatocytes (Pantopoulos et al., 2012). The iron level is tightly regulated in the intracellular compartment, due to its toxicity. From our findings, administration of the alkaloid fraction of *M. jalapa* flowers also increased iron levels in iron deficiency HepG2 cytoplasm. A recent study has indicated that HepG2 and Caco-2 cells treated with ankaferd blood stopper (ABS) have increased intracellular iron levels through the inhibition of HAMP gene expression (Gulec & Gulec, 2018). From this study, we do not know whether or not ABS interacts with the MT-2 protein, as high iron levels in this compound also inhibit the gene expression of TFR, DMT-1, and Ankrd37, which are not related to the MT2–BMP pathway. Therefore, our findings might explain the role of alkaloid fraction of *M. jalapa* flowers in iron metabolism through EPO-MT-2-hepcidin pathway.

Overall, we have documented, for the first time, that the alkaloid fraction of *M. jalapa* flowers up-regulates the EPO levels, TTSPs activity and MT-2 expression in iron deficiency HepG2 cell model, leading to low hepcidin levels and increased intracellular iron levels. However, there were some limitations to our study. At first, we used the *Betanin* pure compound to determine *Betaxanthin* and *Betacyanin* levels, as these compounds are unavailable on the market, while *Betanin* is the precursor of both compounds. In the TTSPs activity assay, we used the Boc-Gln-Ala-Arg-AMC substrate, which can be cleaved not only by MT-2 but also by other TTSPs family members. However, the MT-2 protein expression results are consistent with the TTSPs activity. Furthermore, we did not measure the protein expression and dissociation affinity of BMP and BMPR, which play important roles in hepcidin modulation for iron metabolism.

5. Conclusions

The alkaloid fraction of *M. jalapa* flowers exhibited low cytotoxicity (IC_{50} = 100.21 ± 5.67 ppm) in HepG2 cells. The alkaloid fraction, containing *Indicaxanthin* and *Miraxanthin-V,* increased EPO levels, membrane and soluble TTSPs activities and MT-2 expression, decreased hepcidin levels, and increased intracellular iron levels in iron deficiency HepG2 cell model. In the future, we intend to isolate *Betaxanthin* and its derivatives from *M. jalapa* flowers. To verify the EPOR, MT-2, and TTSPs family member expression, we will use quantitative PCR for gene expression and Western Blotting for protein expression. We will also assess small molecule–protein interactions by using surface plasmon resonance to determine the association and dissociation affinities of *Betaxanthin* and its derivatives with EPOR.

Fundings

This study received funding from the Ministry of Research, Technology and Higher Education of the Republic of Indonesia and the Institute of Research and Community Services, Universitas Sebelas Maret, Indonesia, with Grant No 221.1/UN27.22/HK.07.00/2021 and 254/UN27.22/PT.01.03/2022, respectively.

CRediT authorship contribution statement

Yuliana Heri Suselo: Data curation, Formal analysis, Investigation, Writing – original draft. **Dono Indarto:** Conceptualization, Data curation, Formal analysis, Methodology, Supervision, Writing – review & editing. **Brian Wasita:** Data curation, Methodology, Validation, Writing – review & editing. **Hartono Hartono:** Formal analysis, Methodology, Supervision, Writing – review & editing.

Declaration of Competing Interest

The authors declare that they have no known competing financial interests or personal relationships that could have appeared to influence the work reported in this paper.

Acknowledgments

The authors would like to thank to the Institute of Research and Community Services, Universitas Sebelas Maret, Indonesia, for approval of the research proposal.

Appendix A. Supplementary material

Supplementary data to this article can be found online at https://doi.org/10.1016/j.sjbs.2022.103508.

References

Adiparadana, D., Suselo, Y.H., Balgis, 2015. Screening Indonesian Medical Plants Phytochemistry Using Molecular Docking as Hepcidin Antagonis in Iron Deficiency Anemia. Nexus KedokteranTranslasional 4 (2), 1–15. Retrieved from https://jurnal.fk.uns.ac.id/index.php/Nexus-Kedokteran-Translasional/article/view/785.

Agency of Health Research and Development. 2019. Indonesia Basic Health Research 2018. In: Agency of Health Research and Development. Retrieved from http://labdata.litbang.kemkes.go.id/.

Agency of Health Research and Development. 2013. Indonesia Basic Health Research 2013. https://doi.org/10.1007/s13398-014-0173-7.2.

Al-Snafi, A.E., Talab, T.A., Jabbar, W.M., Alqahtani, A.M., 2021. Chemical constituents and pharmacological activities of Mirabilis jalapa- A review. International Journal of Biological and Pharmaceutical Sciences Archive 1 (2), 034–045. https://doi.org/10.30574/ijbpsa.2021.1.2.0303.

Bajbouj, K., Shafarin, J., Hamad, M., 2018. High-dose deferoxamine treatment disrupts intracellular iron homeostasis, reduces growth, and induces apoptosis in metastatic and nonmetastatic breast cancer cell lines. Technol. Cancer Res. Treat. 17, 1–11. https://doi.org/10.1177/1533033818764470.

Bedessem, B., 2015. Effects of the Hypoxia-Mimetic Agents DFO and CoCl2 on HeLa-Fucci Cells. Cell Biology & Cell Metabolism 2 (1), 1–8. https://doi.org/10.24966/cbcm-1943/100004.

Béliveau, F., Tarkar, A., Dion, S.P., Désilets, A., Ghinet, M.G., Boudreault, P.L., Leduc, R., 2019. Discovery and Development of TMPRSS6 Inhibitors Modulating Hepcidin Levels in Human Hepatocytes. Cell Chem. Biol. 26 (11), 1559–1572. e9. https://doi.org/10.1016/j.chembiol.2019.09.004.

Bisswanger, H., 2014. Enzyme assays. Perspect. Sci. 1 (1–6), 41–55. https://doi.org/10.1016/j.pisc.2014.02.005.

Bregman, D.B., Morris, D., Koch, T.A., He, A., Goodnough, L.T., 2013. Hepcidin levels predict nonresponsiveness to oral iron therapy in patients with iron deficiency anemia. Am. J. Hematol. 88 (2), 97–101. https://doi.org/10.1002/ajh.23354.

Camaschella, C., Nai, A., Silvestri, L., 2020. Iron metabolism and iron disorders revisited in the hepcidin era. Haematologica 105 (2), 260–272. https://doi.org/10.3324/haematol.2019.232124.

Coy-Barrera, E., 2020. Analysis of betalains (betacyanins and betaxanthins). Recent Advances in Natural Products Analysis 593–619. https://doi.org/10.1016/b978-0-12-816455-6.00017-2.

Damalanka, V.C., Janetka, J.W., 2019. Recent progress on inhibitors of the type II transmembrane serine proteases, hepsin, matriptase and matriptase-2. Future Med. Chem. 11 (7), 743–769. https://doi.org/10.4155/fmc-2018-0446.

dos Santos, E.T., Pereira, M.L.A., da Silva, C.F.P.G., Souza-Neta, L.C., Geris, R., Martins, D., Batista, R., 2013. Antibacterial activity of the alkaloid-enriched extract from Prosopis juliflora pods and its influence on in Vitro ruminaldigestion. Int. J. Mol. Sci. 14 (4), 8496–8516. https://doi.org/10.3390/ijms14048496.

Fernández-López, J.A., Giménez, P.J., Angosto, J.M., Moreno, J.I., 2012. A process of recovery of a natural yellow colourant from Opuntia fruits. Food Technol. Biotechnol. 50 (2), 246–251.

Fleming, M. D. 2008. The regulation of hepcidin and its effects on systemic and cellular iron metabolism. Hematology / the Education Program of the American Society of Hematology. American Society of Hematology. Education Program, (May), 151–158. https://doi.org/10.1182/asheducation-2008.1.151.

Frýdlová, J., Pøikryl, P., Truksa, J., Falke, L.L., Du, X., Gurieva, I., Krijt, J., 2016. Effect of Erythropoietin, Iron Deficiency and Iron Overload on Liver Matriptase-2 (TMPRSS6) Protein Content in Mice and Rats. PLoS One 11 (2), 1–17. https://doi.org/10.1371/journal.pone.0148540.

Fung, E., Nemeth, E., 2013. Manipulation of the hepcidin pathway for therapeutic purposes. Haematologica 98 (11), 1667–1676. https://doi.org/10.3324/haematol.2013.084624.

Garrido, P., Ribeiro, S., Fernandes, J., Vala, H., Rocha-Pereira, P., Bronze-da-Rocha, E., Reis, F., 2015. Resistance to recombinant human erythropoietin therapy in a rat model of chronic kidney disease associated anemia. Int. J. Mol. Sci. 17 (1). https://doi.org/10.3390/ijms17010028.

Gogoi, J., Nakhuru, K.S., Policegoudra, R.S., Chattopadhyay, P., Rai, A.K., Veer, V., 2016. Isolation and characterization of bioactive components from Mirabilis jalapa L. radix. J. Tradit. Complement. Med. 6 (1), 41–47. https://doi.org/10.1016/j.jtcme.2014.11.028.

Gulec, A., Gulec, S., 2018. Ankaferd Influences mRNA Expression of Iron-Regulated Genes During Iron-Deficiency Anemia. Clin. Appl. Thromb. Hemost. 24 (6), 960–964. https://doi.org/10.1177/1076029617737838.

Gurieva, I., Frýdlová, J., Rychtarčíková, Z., Vokurka, M., Truksa, J., Krijt, J., 2017. Erythropoietin administration increases splenic erythroferrone protein content and liver TMPRSS6 protein content in rats. Blood Cell Mol. Dis. 64, 1–7. https://doi.org/10.1016/j.bcmd.2017.02.007.

Hawula, Z.J., Wallace, D.F., Subramaniam, V.N., Rishi, G., 2019. Therapeutic advances in regulating the hepcidin/ferroportin axis. Pharmaceuticals 12 (4), 1–22. https://doi.org/10.3390/ph12040170.

Ikawati, Z., Sudjadi, & Sismindari. 2006. Cytotoxicity against tumor cell lines of a ribosome-inactivating protein (RIP)-like protein isolated from leaves of Mirabilis jalapa L. Malaysian Journal of Pharmaceutical Sciences, 4(1), 31–41. Retrieved from http://web.usm.my/mjps/MJPS 4(1) 2006/MJPS 4.1.4.pdf.

Katsarou, A., Pantopoulos, K., 2018. Hepcidin therapeutics. *Pharmaceuticals* 11 (4), 1–30. https://doi.org/10.3390/PH11040127.

Khan, M.I., Giridhar, P., 2015. Plant betalains: Chemistry and biochemistry. Phytochemistry 117, 267–295. https://doi.org/10.1016/j.phytochem.2015.06.008.

Lavanya, V., Thamaraiselvi, S.P., Uma, D., 2019. Studies on Extraction of Betalain Pigments by Different Solvents and Assessing Antioxidant Activity of Bougainvillea spectabilis and Celosia argentea Flowers. Madras Agricultural Journal 106 (1–3), 104–108. https://doi.org/10.29321/maj.2019.000230.

Livingstone, J., 2001. Natural compounds in cancer therapy. International Journal Of Pharmaceutical Medicine 15. https://doi.org/10.2165/00124363-200110000-00017.

Mangold, M., Gütschow, M., Stirnberg, M., 2018. A short peptide inhibitor as an activity-based probe for matriptase-2. Pharmaceuticals 11 (2). https://doi.org/10.3390/ph11020049.

Maulina, D., Sumitro, S.B., Amin, M., Lestari, S.R., 2018. Identification of bioactive compounds from Mirabilis jalapa L. (Caryophyllales: Nyctaginaceae) extracts as biopesticides and their activity against the immune response of Spodoptera litura F. (Lepidoptera: Noctuidae). J. Biopest. 11 (2), 89–97.

Middleton, S.A., Barbone, F.P., Johnson, D.L., Thurmond, R.L., You, Y., McMahon, F.J., Jolliffe, L.K., 1999. Shared and unique determinants of the erythropoietin (EPO) receptor are important for binding EPO and EPO mimetic peptide. J. Biol. Chem. 274 (20), 14163–14169. https://doi.org/10.1074/jbc.274.20.14163.

Ministry of Health. 2017. Farmakope Herbal Indonesia (2nd ed.). Jakarta.

Moçanu, G.D., Nistor, O.V., Andronoiu, D.G., Ceclu, L., Gheonea, I.D., Mihalcea, L., Patrașcu, L., 2020. Effects of drying methods on quality parameters of potato and red beetroot purée with Lactobacillus delbrueckii. Journal of Food and Nutrition Research 59 (1), 23–34.

Nai, A., Rubio, A., Campanella, A., Gourbeyre, O., Artuso, I., Bordini, J., Meynard, D., 2016. Limiting hepatic Bmp-Smad signaling by matriptase-2 is required for erythropoietin-mediated Hepcidin suppression in mice. Blood 127 (19), 2327–2336. https://doi.org/10.1182/blood-2015-11-681494.

Naqvi, S.F.H., Husnain, M., 2020. Betalains: Potential drugs with versatile phytochemistry. Crit. Rev. Eukaryot. Gene Expr. 30 (2), 169–189. https://doi.org/10.1615/CritRevEukaryotGeneExpr.2020030231.

Pantopoulos, K., Porwal, S.K., Tartakoff, A., Devireddy, L., 2012. Mechanisms of mammalian iron homeostasis. Biochemistry 51 (29), 5705–5724. https://doi.org/10.1021/bi300752r.

Piattelli, M., Minale, L., Nicolaus, R., 1965. Pigments of centrospermae—V.: Betaxanthins from Mirabilis jalapa L. 4 (1), 817–823 https://doi.org/10.16309/j.cnki.issn.1007-1776.2003.03.004.

Polturak, G., Heinig, U., Grossman, N., Battat, M., Leshkowitz, D., Malitsky, S., Aharoni, A., 2018. Transcriptome and Metabolic Profiling Provides Insights into Betalain Biosynthesis and Evolution in Mirabilis jalapa. Mol. Plant 11 (1), 189–204. https://doi.org/10.1016/j.molp.2017.12.002.

Rainville, N., Jachimowicz, E., Wojchowski, D.M., 2016. Targeting EPO and EPO receptor pathways in anemia and dysregulated erythropoiesis. Expert Opin. Ther. Targets 20 (3), 287–301. https://doi.org/10.1517/14728222.2016.1090975.

Rawlings, N.D., 2020. Twenty-five years of nomenclature and classification of proteolytic enzymes. Biochimica et Biophysica Acta - Proteins and Proteomics 1868, (2). https://doi.org/10.1016/j.bbapap.2019.140345 140345.

Sadowska-Bartosz, I., Bartosz, G., 2021. Biological properties and applications of betalains. Molecules 26 (9), 1–36. https://doi.org/10.3390/molecules26092520.

Sharathna, P., Alisha, V., Sasikumar, P., Ajesh, V., Ayisha, F., Shibi, I.G., et al., 2021. Mirabijalones S-W, rotenoids from rhizomes of white Mirabilis jalapa Linn. and their cell proliferative studies. Phytochem. Lett. 44 (July), 178–184. https://doi.org/10.1016/j.phytol.2021.06.017.

Singh, V.K., Kumar, N., Kalsan, M., Saini, A., 2013. In silico Designing and Optimization of EPO Mimetic Using Combinatorial Library. International Journal of Science and Research 14 (1), 2319–7064. Retrieved from www.ijsr.net.

Stevens, G.A., Finucane, M.M., De-Regil, L.M., Paciorek, C.J., Flaxman, S.R., Branca, F., Ezzati, M., 2013. Global, regional, and national trends in haemoglobin concentration and prevalence of total and severe anaemia in children and pregnant and non-pregnant women for 1995–2011: A systematic analysis of population-representative data. Lancet Glob. Health 1 (1), 16–25. https://doi.org/10.1016/S2214-109X(13)70001-9.

Stirnberg, M., Maurer, E., Horstmeyer, A., Kolp, S., Frank, S., Bald, T., Gütschow, M., 2010. Proteolytic processing of the serine protease matriptase-2: Identification of the cleavage sites required for its autocatalytic release from the cell surface. Biochem. J 430 (1), 87–95. https://doi.org/10.1042/BJ20091565.

Suselo, Y.H., Alhaqq, A., Indarto, D., 2020. Cathafiline from Cassytha filiformis and BR-Xanthone A from Garcinia mangostana as potential bone morphogenetic protein receptor type i (BMPR-I) inhibitor for iron-refractory iron deficiency

anemia in silico. IOP Conference Series: Materials Science and Engineering 858 (1). https://doi.org/10.1088/1757-899X/858/1/012034.
Suselo, Y. H., Kamil, K., Wulandari, S., & Indarto, D. 2017. Indicaxanthin, Miraxanthin-V, and Hexahydrocurcumin as Potential Erythropoietin Agonist in Silico to Treat Anemia in Chronic Kidney Disease. 2(Hsic). https://doi.org/10.2991/hsic-17.2017.62.
Suselo, Y.H., Wulandari, S., Ayusari, A.A., Indarto, D., 2017b. Hepcidin and Matriptase-2 as a potential biomarker for responsiveness to oral iron supplementation in adolescents female with iron deficiency anemia. Bali Medical Journal 6 (3), 61 https://doi.org/10.15562/bmj.v6i3.722.
Webb, S.L., Sanders, A.J., Mason, M.D., Jiang, W.G., 2011. Type II Transmembrane Serine Protease (TTSP) deregulation in cancer. Frontiers in Bioscience (Landmark Edition) 16 (4), 539–552.
WHO. 2015. The Global Prevalence of Anaemia in 2011. Geneva.
Xu, J.J., Qing, C., Lv, Y.P., Liu, Y.M., Liu, Y., Chen, Y.G., 2010. Cytotoxic Retinoid from Mirabilis jalapa. Chem. Nat. Compd. 46 (5), 792–794. https://doi.org/10.1007/s10600-010-9744-9.
Yotriana, S., Suselo, Y. H., Muthmainah, & Indarto, D. 2018. Miraxanthin-V, Liriodenin and Chitranone are Hepcidin Antagonist in silico for Iron Deficiency Anemia. IOP Conference Series: Materials Science and Engineering, 333(1). https://doi.org/10.1088/1757-899X/333/1/012079.
Zhao, N., Nizzi, C.P., Anderson, S.A., Wang, J., Ueno, A., Tsukamoto, H., Zhang, A.S., 2015. Low intracellular iron increases the stability of Matriptase-2. J. Biol. Chem. 290 (7), 4432–4446. https://doi.org/10.1074/jbc.M114.611913.